ResearchGate

See discussions, stats, and author profiles for this publication at: https://www.researchgate.net/publication/231649663

MCM-41-Supported Organometallic-Derived Nanopalladium as a Selective Hydrogenation Catalyst

ARTICLE *in* THE JOURNAL OF PHYSICAL CHEMISTRY C · MAY 2008

Impact Factor: 4.77 · DOI: 10.1021/jp8007656

CITATIONS
35

READS
32

6 AUTHORS, INCLUDING:

Niladri Maity
King Abdullah University of Science and Te…
11 PUBLICATIONS **91** CITATIONS
SEE PROFILE

Subramanian Ganapathy
CSIR - National Chemical Laboratory, Pune
18 PUBLICATIONS **273** CITATIONS
SEE PROFILE

Sumit Bhaduri
Indian Institute of Technology Bombay
137 PUBLICATIONS **1,944** CITATIONS
SEE PROFILE

Available from: Niladri Maity
Retrieved on: 01 February 2016

MCM-41-Supported Organometallic-Derived Nanopalladium as a Selective Hydrogenation Catalyst

Niladri Maity,[†] Pattuparambil R. Rajamohanan,[||] Subramanian Ganapathy,[||] Chinnakonda S. Gopinath,*[,§] Sumit Bhaduri,*[,‡] and Goutam Kumar Lahiri*[,†]

Department of Chemistry, Indian Institute of Technology-Bombay, Powai, Mumbai 400076, India, Reliance Industries Limited, Swastik Mills Compound, V. N. Purav Marg, Chembur, Mumbai 400071, India, and Catalysis Division and Central NMR Facility, National Chemical Laboratory, Pune 411008, India

Received: January 23, 2008; Revised Manuscript Received: March 11, 2008

Palladium nanocatalysts have been prepared by anchoring $(\eta^3\text{-}C_3H_5)_2Pd_2Cl_2$ onto diamine-functionalized MCM-41 supports followed by reaction with hydrogen under catalytic conditions. The catalyst precursor and used catalyst have been studied by solid-state NMR (^{13}C, ^{29}Si), XPS, and TEM. The organometallic-derived catalyst exhibits the best performance (activity and selectivity) to date toward the selective hydrogenation of industrially relevant *o*- and *m*-chloronitrobenzene to the corresponding chloroaniline derivatives and is distinctly superior to 5% Pd/C. Grazing angle XPS studies reveal that conversion of the tethered molecular species to the nanoparticles of palladium produces a core−shell nanostructure.

Introduction

An actively explored strategy for developing high-performance transition-metal-based heterogeneous catalysts is the use of small metal crystallites or nanocatalysts on organic or inorganic supports.[1,2] Transition-metal nanoparticles are attractive as catalysts due to their high surface-to-volume ratio compared to bulk catalytic materials and the fact that if controlled their surface structures can give rise to high selectivity.[3,4] Organometallic complexes have been extensively studied as precursors of nanocatalysts, but there are only a few reports on high-performance, well-characterized palladium nanocatalysts.[4–10] Among the support materials mesoporous materials such as MCM-41 or SBA-15 are unique as their regular and optimum pore sizes and easy functionalization often result in catalysts of high activity and unusual selectivity.[11–14] Especially noteworthy in the present context is the recent report on the hydrogenation of acetophenone where SBA-15-supported nanopalladium in the presence of proline gives better enantioselectivity than Ultrafine palladium black.[14]

Discovery of a high-performance catalyst for the hydrogenation of substituted nitrobenzene has recently been the subject of much research, and nanoparticles of gold, platinum, cobalt, etc., have been found to have high selectivity and/or activity.[15–17] Efficient hydrogenation of *o*- and *m*-chloronitrobenzene (CNB), with low hydrodehalogenation, is a reaction of considerable industrial importance as the products *o*- and *m*-chloroaniline are intermediates for the commercial manufacture of many pharmaceuticals.[18] The objective therefore is to maximize the yields of *o*- and *m*-chloroaniline and minimize the hydrodehalogenation byproducts nitrobenzene and aniline that are formed due to hydrogenolysis of the carbon−chlorine bond. While there are some reports on the use of platinum catalysts for this reaction, very few studies have been carried out with palladium catalysts.[19] As palladium is cheaper than platinum, there is an obvious need for the development of selective palladium catalysts.

Here we report an easy to synthesize MCM-41-tethered organometallic precursor that generates a palladium nanocatalyst under catalytic hydrogenation conditions. In the hydrogenation of *o*- and *m*-CNB, the nanoparticles show the best performance reported to date for palladium catalysts.

Experimental Details

All preparations and manipulations were performed using standard Schlenk techniques under an atmosphere of argon or nitrogen. 1,2-Diaminocyclohexane, *N*-[3-(trimethoxysilylpropyl)]ethylenediamine ($(CH_3O)_3SiCH_2CH_2CH_2NHCH_2CH_2NH_2$), and (3-chloropropyl)trimethoxysilane ($(CH_3O)_3SiCH_2CH_2CH_2Cl$) were obtained from Aldrich. Nitrobenzene, aniline, *ortho*- and *meta*-chloronitrobenzene (*o*- and *m*-CNB), *ortho*- and *meta*-chloroaniline (*o*- and *m*-chloroaniline), and ethylenediamine were obtained from Merck India Limited. Commercial catalyst Pd (5%) on charcoal was purchased from Spectrochem Limited, India. MCM-41 and $[(\eta^3\text{-}C_3H_5)_2Pd_2Cl_2]$ were synthesized according to the literature procedures.[20,21] A JEOL 1200 EX transmission electron microscope, VG Microtech Multilab ESCA 3000 spectrometer, 400 MHz Varian FT spectrometer (solution), Bruker DRX 500 NMR (solid state), and Micromass Q-ToF mass spectrometer were used for TEM, ESCA, NMR, and mass spectrometric measurements, respectively. Elemental analysis, solution electrical conductivity, and palladium content of fresh and used catalyst **1** were measured by using a Perkin-Elmer 240C elemental analyzer, Systronic 305 conductivity bridge, and 8440 Plasma Laboratory ICP-AES instrument, respectively. The details of the data acquisition techniques for NMR and ESCA measurements have been reported in our earlier publications.[22,23] Synthetic procedures for **1** and the untethered organometallic analogue **3** are given below.

Synthesis of 1. MCM-41 (1 g) preheated under vacuum at 200 °C for 4 h was refluxed with 2 mL of *N*-[3-(trimethoxysilyl)propyl]ethylenediamine and 20 mL of dry toluene at 110 °C for 120 h (Scheme 1). The product was then separated by

* To whom correspondence should be addressed. Phone: +91-22-2576-7159. Fax: +91-22-2572-3480. E-mail: lahiri@chem.iitb.ac.in.
† Indian Institute of Technology-Bombay.
‡ Reliance Industries Limited.
§ Catalysis Division, National Chemical Laboratory.
|| Central NMR Facility, National Chemical Laboratory.

10.1021/jp8007656 CCC: $40.75 © 2008 American Chemical Society
Published on Web 05/29/2008

SCHEME 1: Preparation of precursor of catalyst 1

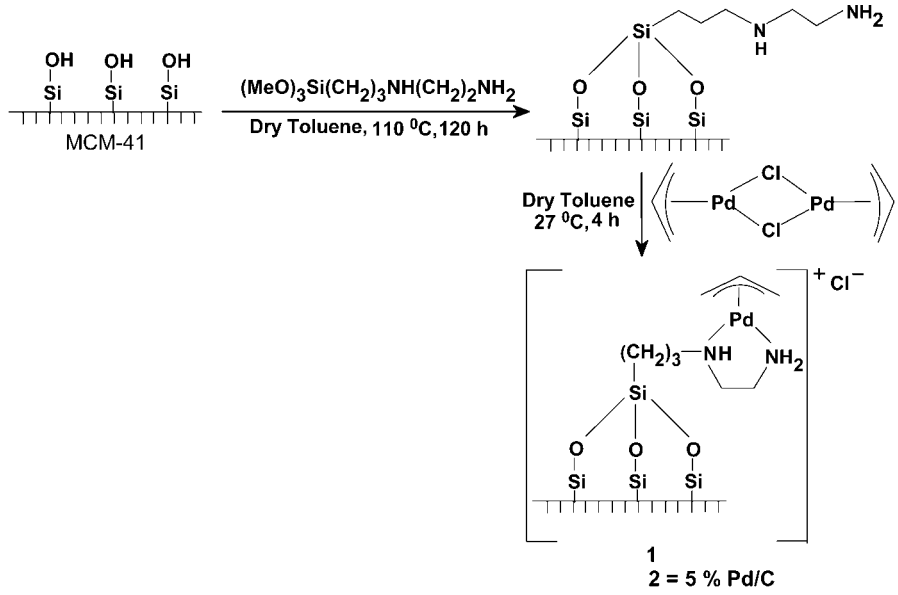

SCHEME 2: Synthesis of Complex 3

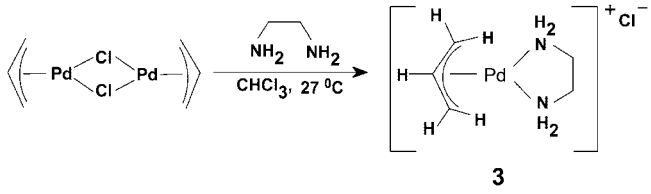

filtration and washed several times with dry toluene followed by dry methanol.

Dried *N*-[3-(trimethoxysilyl)propyl]ethylenediamine-modified functionalized MCM-41 (1 g) was added into the yellow solution of $(\eta^3\text{-}C_3H_5)_2Pd_2Cl_2$ (0.4 g) in dry toluene. The mixture was stirred at 27 °C for 4 h under a nitrogen atmosphere. The solid material was filtered off and washed thoroughly with toluene. The faint yellow material (**1**) thus obtained was stored in a vacuum desiccator. The specific surface area (m^2/g) of **1** is 430, and the maximum cumulative area is 410.

Synthesis of $[(\eta^3\text{-}C_3H_5)Pd(NH_2CH_2CH_2NH_2)]Cl$ (3). A 366 mg (1 mmol) amount of $[(\eta^3\text{-}C_3H_5)_2Pd_2Cl_2]$ was dissolved in 10 mL of $CHCl_3$. A 120 mg amount of ethylenediamine (2 mmol) in 2 mL of $CHCl_3$ was added into the above solution dropwise under stirring at 27 °C over a period of 10 min (Scheme 2). Solvent was then removed by a rotary evaporator at 60 °C. The white material (**3**) thus formed was highly hygroscopic in nature, and it was stored in a vacuum desiccator. Yield = 349 mg (72%). ^{1}H NMR (400 MHz, $(CD_3)_2SO$): δ 5.36−5.26 (m, 1H), 4.57 (br, 4H), 3.84 (d, J = 6.8 Hz, 2 H), 2.72 (d, J = 12 Hz, 2H), 2.49 (s, 4H). ^{13}C NMR (400 MHz, D_2O): δ 114.88, 57.03, 43.91. Anal. Calcd for $C_5H_{13}ClN_2Pd$: C, 24.71; H, 5.39; N, 11.53. Found: C, 24.54; H, 5.33; N, 11.24. MS (ESI): 206.96 (207.01 calcd for $C_5H_{13}N_2Pd$, $[M - Cl]^+$). Molar conductivity [Λ_M ($\Omega^{-1}cm^2\ M^{-1}$)] in H_2O: 110.

The catalytic runs in general were carried out at 27 °C with specified amounts of catalysts and substrates in fixed volumes of methanol in glass vials with magnetic stirring. The glass vial was placed in an autoclave, and a specific hydrogen pressure (Table 3 and Figure 2) was applied. At the end of the catalytic run the reaction mixture was subjected to GC and the extent of conversion was calculated on the basis of the ratio of areas of starting material and product using toluene as an internal standard. Conversions and chemoselectivity of the hydrogenation reactions with different substrates were monitored by the gas chromatographic technique with a FID detector (Shimadzu GC-2014 gas chromatograph) using a capillary column (112-2562 CYCLODEXB, from J&W Scientific, length 60 m, i.d. 0.25 mm, film 0.25 μm). All hydrogenated products were initially identified using authentic commercial samples of the expected products.

TABLE 1: Extent of Functionalization of Supports and Bulk Pd Content in 1

catalyst	silyl group present[a] (mmol/g)	diamine moiety (mmol/g)	bulk palladium[b] (wt %) [mmol/g]
1	1.5[c]	1.5	4.0 [0.4]

[a] Estimated via elemental (C, H, N) analysis. [b] Estimated by ICP-AES. [c] *N*-[3-(Trimethoxysilyl)propyl]ethylenediamine.

Results and Discussion

Synthesis and Characterization of 1. The synthetic procedures adopted for obtaining **1** along with its structural formulation is given in Scheme 1. MCM-41 is first functionalized with *N*-[3-(trimethoxysilyl)propyl]ethylenediamine and then reacted with $(\eta^3\text{-}C_3H_5)_2Pd_2Cl_2$. The amounts of the silyl and amino functionalities as well as palladium loading for **1** are given in Table 1. The silyl and diamine content of **1** are the same, as they must be, but the palladium content is significantly smaller than that of the diamine functionalities. Thus, only a few of the surface diamine functionalities (∼25%) act as ligands, and the rest remain free.

The IR spectra of the diamine-functionalized MCM-41 and **1** show ν_{C-H} but do not provide unambiguous evidence about the molecular structure of the tethered species. This is because unlike carbonyls the organometallic moiety does not have any strong, characteristic absorption. The structural formulation of **1** is therefore based on NMR and XPS studies on the solids and comparison of NMR data with that of the soluble molecular analogue **3** synthesized by treatment of $(\eta^3\text{-}C_3H_5)_2Pd_2Cl_2$ with ethylenediamine (Scheme 2). The solid-state NMR spectra (^{29}Si and ^{13}C) of MCM-41 functionalized with *N*-[3-(trimethoxysilyl)propyl]ethylenediamine and **1** are shown in Figure 1. For comparison, the ^{13}C NMR spectrum of solid $(\eta^3\text{-}C_3H_5)_2Pd_2Cl_2$ is also shown.

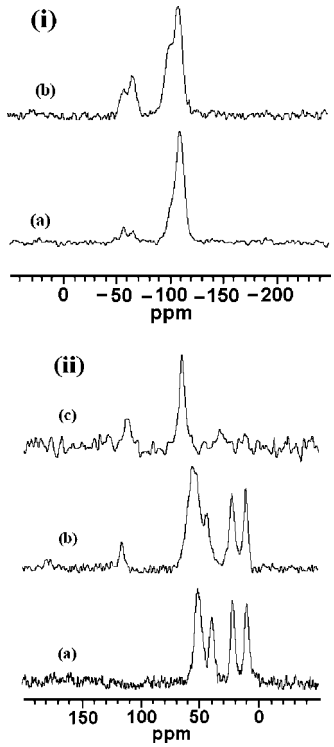

Figure 1. (i) ^{29}Si (CPMAS) NMR of (a) MCM-41 functionalized with $(CH_3O)_3SiCH_2CH_2CH_2NHCH_2CH_2NH_2$ and (b) fresh catalyst **1**. (ii) ^{13}C (CPMAS) NMR spectra of (a) MCM-41 functionalized with $(CH_3O)_3SiCH_2CH_2CH_2NHCH_2CH_2NH_2$, (b) fresh catalyst **1**, and (c) $(\eta^3\text{-}C_3H_5)_2Pd_2Cl_2$.

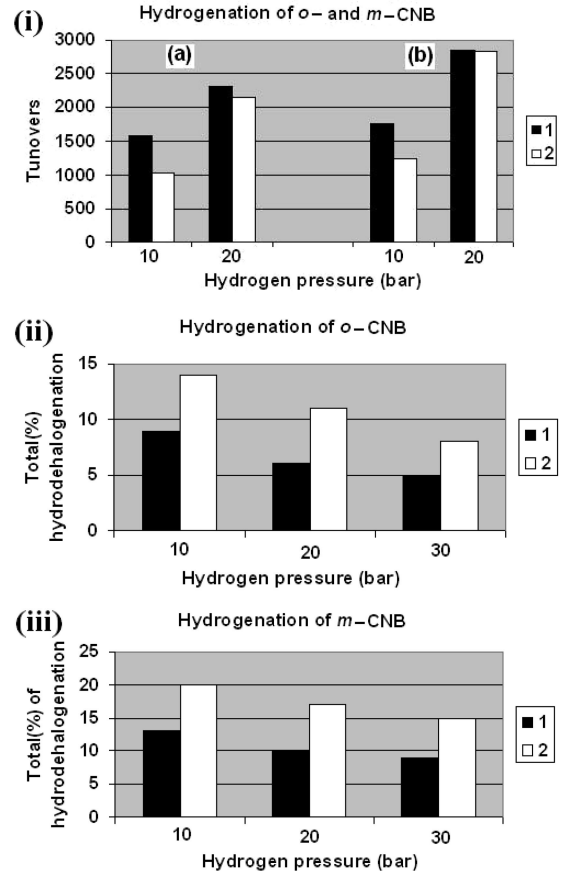

Figure 2. (i) Comparative activity diagram of catalysts **1** and **2** on substrates (a) *o*-CNB and (b) *m*-CNB at 10 and 20 bar hydrogen pressure. (ii) Hydrodehalogenation (nitrobenzene plus aniline) of *o*-CNB. (iii) Hydrodehalogenation (nitrobenzene plus aniline) of *m*-CNB by catalysts **1** and **2** at 10, 20, and 30 bar hydrogen pressure. All catalytic runs were carried out with 70 mg of each catalyst, **1** (2.6×10^{-2} mmol of palladium) and **2** (3.2×10^{-2} mmol of palladium), in 20 mL of methanol with 14.4 g (91.4 mmol) of substrate at 27 °C for 15 min. Also see Table 3.

After reaction with $(CH_3O)_3SiCH_2CH_2CH_2NHCH_2CH_2NH_2$, the intensities of the Q^3 and Q^2 signals [$Q^n = Si(OSi)_n(OH)_{4-n}$ by convention] of MCM-41 are substantially reduced and three strong new signals at $\delta = -49.9$ (T^1), -59.6(T^2), and -68.2(T^3) are observed [$T^m = RSi(OSi)_m(OMe)_{3-m}$ by convention] (Figure 1i.a). The ^{29}Si NMR spectrum of **1** shows two peaks at $\delta = -59.6(T^2)$ and $-68.2(T^3)$ but no observable signal due to T^1 (Table 2) (Figure 1i.b). This is probably because during the metalation process the "Si−O CH_3" linkages of the T^1 silicon atoms are converted into "Si−O−Si" linkages. Coordination of the diamino functionality to the palladium center presumably brings about stereoelectronic changes in the "Si−OCH_3" linkages of the T^1 silicon atoms, making them especially susceptible to hydrolysis. This type of behavior has also been reported for other systems.[22] In Scheme 1 only one type of surface site (T^3) corresponding to each silane reagent is shown, and the T^2 sites are omitted for clarity.

The ^{13}C (CPMAS) spectrum of $(CH_3O)_3SiCH_2CH_2CH_2NHCH_2CH_2NH_2$ treated with MCM-41 shows four different electronic environments for the carbon atoms (Figure 1ii.a),, and the chemical shifts match well with earlier literature reports on similar systems.[22–25] Definitive evidence for the presence of the intact organometallic moiety "(η^3-C_3H_5)Pd" in **1** comes from the clearly identifiable signal of (CH_2***C***HCH_2) at 116.3 ppm (Figure 1ii.b). The other carbon signal, i.e., ***C***H_2CH***C***H_2, appears clearly at 66.3 for $(\eta^3\text{-}C_3H_5)_2Pd_2Cl_2$ (Figure 1ii.c), but in **1**, because it overlaps with other carbon signals, it can be seen only as a shoulder at 56.1. Detailed chemical shift data are given in Table 2.

Catalytic Hydrogenation Reaction. The turnover numbers (turnover frequencies) for nitrobenzene hydrogenation with **1** and **2** (commercial Pd (5%) on carbon) as the catalysts were first measured. The activities of **1** and **2** were found to be comparable, and turnovers (TON) ≈ 6500−7000 (∼110 min^{-1}) were obtained over a period of 1 h (27 °C, 30 bar H_2, nitrobenzene:Pd mole ratio ≈ 10^4:1). In view of their comparable activities toward nitrobenzene, the two catalysts were then subjected to further studies for hydrogenation of *o*- and *m*-CNB (Table 3).

It is clear that **1** indeed is a high-performance catalyst even without optimization of all the reaction parameters. As shown in Figure 2i and Table 3, higher TONs are consistently obtained with **1** in every case. More importantly, it is notably more selective than **2** (Figure 2ii and 2iii). At 20 bar the total amounts of hydrodehalogenated products (%) with **1** and **2** are 6 and 11 for *o*-CNB and 10 and 17 for *m*-CNB. In other words, at 20 bar pressure for *o*-CNB and *m*-CNB the amount of undesirable byproduct with **2** is 1.8 and 1.7 times more than that with **1**. As shown in Figure 2, the higher selectivity of **1** holds at other pressures as well. The observed superior performance of **1** compared to that of **2** may be attributed to a combination of the palladium particle size and support (see later in the paper).

To the best of our knowledge, there are only four other publications where quantitative performance data (turnover and selectivity) on the hydrogenation of *o*-, *m*-, *or p*-CNB using palladium-based catalytic systems are given.[19,26–28] Out of these, in two reports the substrate used is *p*-CNB, which rules out any meaningful comparison between the performances of these catalytic systems and that of **1**.[27,28]

TABLE 2: Solid-State ^{29}Si and ^{13}C NMR Chemical Shift Data

system	chemical shifts (ppm) ^{29}Si	^{13}C
MCM-41	$-110.7(Q^4)$, $-100.9(Q^3)$, $-91.8(Q^2)$	
MCM-41$-(CH_3O)_3SiCH_2CH_2CH_2NHCH_2CH_2NH_2$	$-111.4(Q^4)$, $-102.1(Q^3)$, -49.9 (T^1), $-59.6(T^2)$, $-68.2(T^3)$	50.9 ($-Si-O\mathit{C}H_3$, $-\mathit{C}H_2-NH-\mathit{C}H_2$), 39.4 ($-\mathit{C}H_2-NH_2$), 21.7 ($Si-CH_2-\mathit{C}H_2-CH_2$), 9.4 ($-Si-\mathit{C}H_2-CH_2$)
$(\eta^3\text{-}C_3H_5)_2Pd_2Cl_2$		112.3 ($CH_2-\mathit{C}H-CH_2$), 66.3 ($\mathit{C}H_2-CH_2-\mathit{C}H_2$)
1	$111.6(Q^4)$, $-102.9(Q^3)$, $-59.6(T^2)$, $-68.2(T^3)$	116.3 ($CH_2-\mathit{C}H-CH_2$), 56.1 ($\mathit{C}H_2-CH_2-\mathit{C}H_2$), 52.8 ($-Si-O\mathit{C}H_3$, $-\mathit{C}H_2-NH-\mathit{C}H_2$), 44.5 ($-\mathit{C}H_2-NH_2$), 21.7 ($Si-CH_2-\mathit{C}H_2-CH_2$), 9.4 ($-Si-\mathit{C}H_2-CH_2$)

TABLE 3: Selective Reduction of Chloronitrobenzenes[a]

catalyst	substrate	pressure (bar)	TON (TOF min^{-1})	chloroaniline (%)	aniline (%)	nitrobenzene (%)
1	*o*-CNB	10	1582 (105)	92	6.5	1.5
		20	2320 (155)	94	5	1
		30	3164 (211)	95	5	0
	m-CNB	10	1758 (117)	87	12	1
		20	2847 (190)	90	10	0
		30	3515 (234)	91	9	0
2	*o*-CNB	10	1028 (68)	86	12	2
		20	2142 (143)	89	10	1
		30	2856 (190)	92	8	0
	m-CNB	10	1230 (82)	80	19	1
		20	2827 (188)	83	17	0
		30	3164 (190)	85	15	0

[a] All catalytic runs were carried out with 70 mg of each catalyst, **1** (2.6×10^{-2} mmol of palladium) and **2** (3.2×10^{-2} mmol of palladium), in 20 mL of methanol under hydrogen pressures of 10, 20, and 30 bar at 27 °C for 15 min. The amount of substrate (*o*-CNB and *m*-CNB) used was 14.4 g (91.4 mmol).

Hydrogenation of *o*- and *m*-CNB using Pd/C has been studied in *ionic liquid* and methanol.[19] Although the extent of hydrodehalogenation in ionic liquid at 100 °C is minimal, the turnover frequencies (TOF, min^{-1} bar^{-1}) for *o*- and *m*-CNB are only 0.4 and 0.6. In contrast, with **1** as the catalyst, even at a much lower temperature (27 °C) the TOFs, 7.7 and 9.5, are more than an order of magnitude higher. Hydrogenation of only *o*-CNB at 250 °C using Pd/TiO_2 has also been reported.[26] However, quantitative data on TOF are not given, and the reported selectivity (93.6%) is marginally less than that of **1**. Finally, even compared to the platinum nanocatalyst of high selectivity recently reported by us, catalyst **1** is almost an order of magnitude more active.[16]

The recyclibility of **1** in terms of loss in activity and loss in palladium content has been studied using the same catalyst for nitrobenzene hydrogenation in three successive batches. Over three batches the total amount of aniline produced is 260 mmol. This is accompanied by a 0.003 mmol loss in palladium, i.e., ≤15% palladium content of the fresh catalyst is lost for a total turnover of ∼10 000. As measured by TON, the activity of the catalyst in the third batch is ∼50% of that of the first batch. As discussed below, there are observable changes in the catalyst microstructure after a significant number of turnovers, and this partial loss in activity is probably due to a combination of palladium loss coupled with the change in microstructure.

For nitrobenzene hydrogenation XPS analyses of fresh and used **1** have been carried out to probe the change in the oxidation state of palladium due to exposure to hydrogen. The fresh catalyst (Figure 3) shows Pd 3d core levels at a characteristic

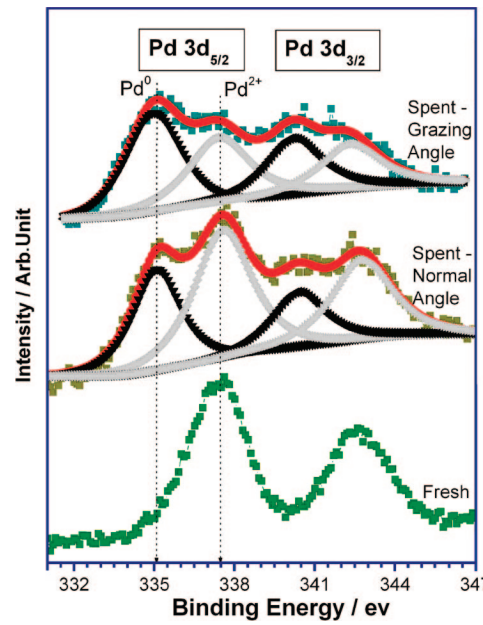

Figure 3. Normal and grazing angle XPS results from the Pd 3d core levels of spent (used) catalyst **1**. XPS result on fresh catalyst is shown for comparison.

binding energy (BE) of Pd^{2+} (Pd $3d_{5/2}$ at 337.5 ± 0.1 eV). With the spent catalyst at a normal emission angle, the Pd 3d core level shows features due to both Pd metal as well as Pd^{2+}. Interestingly, catalysts exposed to hydrogen for different reaction times (nitrobenzene reduction, 1000 ≥ TON ≥ 50) exhibit

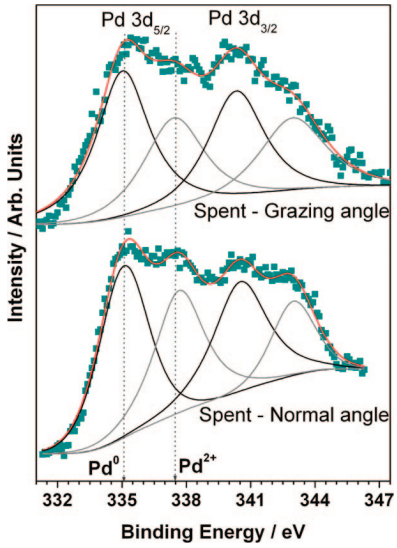

Figure 4. Normal and grazing angle XPS results from the Pd 3d core levels of spent catalyst **1** after 1000 TON. Compared to Figure 3, spent catalyst after higher TON shows more Pd/Pd^{2+} on the surface, which supports the proposed core−shell model.

qualitatively similar Pd 3d core level results. To investigate this aspect further, the spent catalysts have been subjected to grazing angle incidence XPS which helps to identify the occupancy of any particular species exclusively at the surface. From normal angle to grazing angle of incidence, the amount of Pd metal increases significantly at the cost of Pd^{2+} (Figure 3). However, Pd^{2+} does not completely disappear even in a catalyst after ~1000 turnovers (Figure 4). These results indicate that the reduced palladium particles retain Pd^{2+} in the core.

An alternative mechanism, which involves surface oxidation of Pd(0) to PdO during or before XPS analysis, may be ruled out for the following reason. If surface oxidation happens before or during XPS analysis, more Pd^{2+} should have been observed on the top layers at the grazing angle of incidence and not in the inner core at the normal angle of incidence. The experimental observations are however just the opposite; there is more metallic Pd on the surface and Pd^{2+} in the core.

Many TEM micrographs of the fresh and used catalysts were recorded, and a few representative ones that are of relevance to the comparative performance of **1** and **2** are shown in Figure 5. The TEM image of the used catalyst with relatively low turnovers (TON ≤ 500) is similar to that of the fresh catalyst. Both the fresh and the used catalyst show the characteristic MCM-41 fringes, and no palladium particles outside the pores can be seen in either of them (Figure 5a and 5b). The TON in the comparative studies between **1** and **2** ranges from ~1000 to 3500 (see Table 3), and for catalyst **1** after ~2500 turnovers Pd particles (<25 nm) outside the pores can be seen (Figure 5c). However, for catalyst **2** under comparable conditions much larger agglomerates of palladium (Figure 5d) at the edges of the carbon particles are seen and some of the aggregates are ≥300 nm.

The bulk palladium concentrations of **1** and **2** are similar, but the numbers of Pd particles outside the pores of MCM-41 are considerably fewer and also much smaller. It is therefore reasonable to assume that some of the palladium nanoparticles are retained within the pores. Presumably the palladium crystallites both inside and outside the pores are catalytically active though their activities and selectivities probably differ.

On the basis of the XPS and TEM results, as shown in Scheme 3, a likely mechanism for conversion of the supported

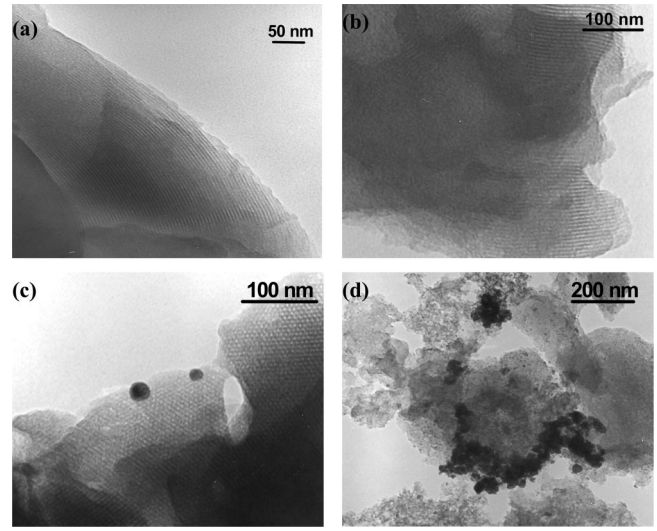

Figure 5. TEM images of (a) fresh catalyst **1**, (b) used catalyst **1**, turnovers ≤ 500, and (c and d) used catalysts **1** and **2**, respectively, after turnovers ≈ 2500.

SCHEME 3: Representation of Formation of the Pd(II) Core with Pd(0) in Used Catalyst 1

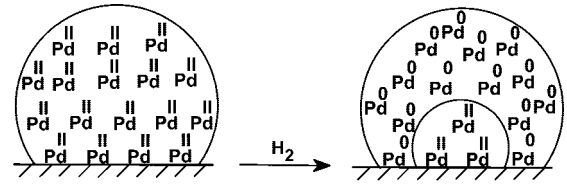

complex to surface-supported palladium nanocatalyst may be postulated. Under catalytic conditions unsaturated Pd^{2+} and Pd^0 centers are formed. Because the diamine ligand is a strong σ donor and Pd^0 is electron rich, the Pd^0 sites are *not* strongly bound to the ligand and can leave the ligand to coalesce together on the neighboring Pd^{2+} centers. This creates a core−shell-type structure within the pore of the used catalyst. A few of the diamino tether groups remain ligated to the residual Pd^{2+} sites on the surface, and the others remain free or weakly interacting with Pd^0 centers.

Clearly the above-mentioned model is applicable only for catalyst with relatively few turnovers (TON ≤ 1000). As the TON increases, the palladium particles coalesce and form larger agglomerates and some of it, as evidenced by TEM, moves out of the pores of MCM-41. However, as mentioned earlier, TEM also shows that the extent of agglomeration is much higher in **2**. Presumably, in **1** the organometallic precursor being confined within the pores of MCM-41 (fringe width ≈ 3 nm) generates palladium nanoparticles of restricted mobility. In contrast, for **2** where high surface area carbon is the support there is no such restriction on mobility and agglomerations of the palladium particles with loss of nanostructure are considerably more extensive.

The better performance of **1** over **2** could therefore be reasonably ascribed to the presence and longer life of palladium nanoparticles in **1**. It is to be noted that restricted mobility for platinum nanoparticles on MCM-41, as opposed to fumed silica, was earlier reported by us and shown to lead to higher selectivity, including enantioselectivity.[12] The question of whether or not the spent catalyst still retains its higher selectivity and the proposed core−shell structure after much higher TON (~10 000) will be addressed in our future work.

Conclusions

We described a simple method for tethering a palladium allyl complex onto MCM-41 and full characterization of the resultant material. This material is an effective precursor of a high-performance catalyst for hydrogenation of *o*- and *m*-chloronitrobenzene with low dehydrohalogenation. XPS and TEM analyses indicate a core−shell structure for the nanoparticles consisting of a Pd^{2+} core covered by a shell of palladium metal.

Acknowledgment. Financial assistance from Reliance Industries Limited, Mumbai and Council of Scientific and Industrial Research, New Delhi, India is gratefully acknowledged.

References and Notes

(1) Astruc, D.; Lu, F.; Aranzaes, J. R. *Angew. Chem., Int. Ed.* **2005**, *44*, 7852.

(2) Thomas, J. M.; Raja, R.; Lewis, D. W. *Angew. Chem., Int. Ed.* **2005**, *44*, 6456.

(3) Narayanan, R.; El-Sayed, M. A. *J. Phys. Chem. B* **2005**, *109*, 12663.

(4) Somorjai, G. A.; Contreras, A. M.; Montano, M.; Rioux, R. M. *Proc. Natl. Acad. Sci. U.S.A.* **2006**, *103*, 10577.

(5) Copéret, C.; Chabanas, M.; Saint-Arroman, R. P.; Basset, J. -M. *Angew. Chem., Int. Ed.* **2003**, *42*, 156.

(6) Guzman, J.; Gates, B. C. *Dalton Trans.* **2003**, 3303.

(7) Braunstein, P.; Oro, L. A.; Raithby, P. R. *Metal Clusters in Chemistry*; Wiley-VCH: Weinheim, 1999.

(8) Lee, H.-Y.; Ryu, S.; Kang, H.; Jun, Y.-W. *Cheon, J. Chem. Commun.* **2006**, 1325.

(9) Mehnert, C. P.; Weaver, D. W.; Ying, J. Y. *J. Am. Chem. Soc.* **1998**, *120*, 12289.

(10) Yang, H.; Zhang, G.; Hong, X.; Zhu, Y. *J. Mol. Catal. A: Chem.* **2004**, *210*, 143.

(11) Li, C.; Zhang, H.; Jiang, D.; Yang, Q. *Chem. Commun.* **2007**, 547.

(12) Basu, S.; Mapa, M.; Gopinath, C. S.; Doble, M.; Bhaduri, S.; Lahiri, G. K. *J. Catal.* **2006**, *239*, 154.

(13) Hungria, A. B.; Raja, R.; Adams, R. D.; Captain, B.; Thomas, J. M.; Midgley, P. A.; Golovko, V.; Johnson, B. F. G. *Angew. Chem., Int. Ed.* **2006**, *45*, 4782.

(14) Chen, X.; Lou, Z.; Qiao, M.; Fan, K.; Tsang, S. C.; He, H. *J. Phys. Chem. C* **2008**, *112*, 1316.

(15) Corma, A.; Serna, P. *Science* **2006**, *313*, 332.

(16) Maity, P.; Basu, S.; Bhaduri, S.; Lahiri, G. K. *Adv. Synth. Catal.* **2007**, *349*, 1955.

(17) Raja, R.; Golovko, V. B.; Thomas, J. M.; Berenguer-Murcia, A.; Zhou, W.; Xie, S.; Johnson, B. F. G. *Chem. Commun.* **2005**, 2026.

(18) Blaser, H.-U. ; Siegrist, U.; Steiner, H.; Studer, M. In *Fine Chemicals through Heterogeneous Catalysis*; Sheldon, R. A., Bekkum, H. V. , Eds.; Wiley-VCH: Weinheim, 2001; pp *389* 406.

(19) Xu, D.-Q.; Hu, Z.-Y.; Li, W.-W.; Luo, S.-P.; Xu, Z.-Y. *J. Mol. Catal. A: Chem.* **2005**, *235*, 137.

(20) Beck, J. S.; Vartuli, J. C.; Roth, W. J.; Leonowicz, M. E.; Kresge, C. T.; Schmitt, K. D.; Chu, C. T.-W.; Olson, D. H.; Sheppard, E. W.; McCullen, S. B.; Higgins, J. B.; Schlenker, J. L. *J. Am. Chem. Soc.* **1992**, *114*, 10834.

(21) Tatsuno, Y.; Yoshida, T.; Seiotsuka, *Inorg. Synth.* **1990**, *28*, 342.

(22) Maity, N.; Basu, S.; Mapa, M.; Rajamohanan, P. R.; Ganapathy, S.; Gopinath, C. S.; Bhaduri, S.; Lahiri, G. K. *J. Catal.* **2006**, *242*, 332.

(23) Wiench, J. W.; Avadhut, Y. S.; Maity, N.; Bhaduri, S.; Lahiri, G. K.; Pruski, M.; Ganapathy, S. *J. Phys. Chem. B* **2007**, *111*, 3877.

(24) Zhang, C.; Zhou, W.; Liu, S. *J. Phys. Chem. B* **2005**, *109*, 24319.

(25) Ek, S.; Iiskola, E. I.; Niinistö, L.; Vaittinen, J.; Pakkanen, T. T.; Root, A. *J. Phys. Chem. B* **2004**, *108*, 11454.

(26) Xu, Q.; Liu, X.-M.; Chena, J.-R.; Li, R.-X.; Li, X.-J. *J. Mol. Catal. A: Chem.* **2006**, *260*, 299.

(27) Yu, Z.; Liao, S.; Xu, Y.; Yang, B.; Yu, D. *J. Mol. Catal. A: Chem.* **1997**, *120*, 247.

(28) Hao, Y.-Z.; Li, Z.-X.; Tian, J.-L. *J. Mol. Catal. A: Chem.* **2007**, *265*, 258.

JP8007656